

## Defects and mass transport in rutile-structured fluorides. II. Computer simulation

A. N. Cormack

*New York State College of Ceramics at Alfred University, Alfred, New York 14802*

C. R. A. Catlow

*Department of Chemistry, University of Keele, Keele, Staffordshire ST5 5BG, United Kingdom*

S. Ling\*

*Henry Krumb School of Mines, Columbia University, New York, New York 10027*

(Received 26 January 1989)

We report the results of a detailed atomistic computer-simulation study of defect structure and energetics in doped and undoped  $\text{MnF}_2$  and  $\text{MgF}_2$ . Our calculations, using improved interatomic potentials over earlier studies, also take into account the anisotropy in the structure. We predict anion Frenkel disorder to predominate intrinsically, but find that the anion interstitial adopts a more complex split-interstitial structure, involving a lattice anion, instead of merely sitting in a straightforward interstice. This complex defect structure is found to associate strongly with trivalent dopants, the association giving rise to low-symmetry dipolar structures. Our calculations of anion-migration activation energies are consistent with an interstitial mechanism. Further comparisons between our calculations and experiment are presented.

### I. INTRODUCTION

Studies of the defect structure of  $\text{MnF}_2$  and  $\text{MgF}_2$  crystals are of considerable interest, since these crystals have the tetragonal rutile structure and therefore must show anisotropy in their defect-transport processes. The preceding paper<sup>1</sup> has made a study, not only of ionic conductivity, but also of low-temperature dielectric relaxation, particularly in trivalent-ion ( $\text{Er}^{3+}$  and  $\text{Y}^{3+}$ )-doped  $\text{MnF}_2$ , as a function of crystallographic orientation. A striking result reported is the presence of dielectric-loss peaks of low activation energies ( $\sim 7$ – $50$  meV). Such loss peaks are not likely to be controlled by defect jumps on the scale of lattice distances, but are more likely due to the reorientation of an "off-center," or more generally, an "off-symmetry," type of defect configuration.

The rutile-structured fluorides are strongly ionic and it should, therefore, be possible to perform reliable computer-simulation studies on them, using the techniques that have been applied with such success to the alkali halides<sup>2,3</sup> and the alkaline-earth fluorides.<sup>4</sup> In fact, such a computer-simulation study was carried out earlier by Catlow *et al.*<sup>5</sup> However, this study utilized the simulation code HADES II, which was designed for crystals with cubic symmetry and, therefore, could not take fully into account the dielectric anisotropy of the continuum component of the simulation. The present study is a reexamination of the problem using a code which was designed to handle noncubic crystals. In addition, F-F short-range potentials used in these calculations, obtained from an extensive study of the alkaline-earth fluorides,<sup>4</sup> are regarded as superior to those employed in the earlier work. Using these improved procedures, we have calculated intrinsic defect-formation and migration energies

and also examined the question of off-symmetry defects involving trivalent cation dopants.

### II. METHODS AND POTENTIALS

We use the standard two-body Mott-Littleton procedures embodied in the CASCADE code, developed by Leslie,<sup>6</sup> which is closely related to the HADES III code.<sup>7</sup> In this approach the crystal is divided into two regions. The inner region, called region I, immediately surrounds the defect, containing typically 100–150 ions. This region is treated atomistically, following the Born model, using pairwise interatomic potentials. The outer region, called region II, is treated as a dielectric continuum whose polarization is found from the Mott-Littleton theory. An interface region is included for consistency between the two different approaches. An important part of the defect energy is the reequilibration of the structure in response to differences in interatomic potential associated with the defect. This is done by minimizing the energy of region I as a function of (explicit) atomic position, subject to the constraint that region II also be in equilibrium. Reviews of both methodology and achievements of these simulation programs are available in the monograph edited by Catlow and Mackrodt.<sup>8</sup> In the CASCADE and HADES III programs, full allowance is made of any anisotropy that might arise from either the crystal symmetry or the lower-symmetry defect structure. The earlier work of Catlow *et al.*<sup>5</sup> used a simpler simulation code, HADES II, which imposed cubic-symmetry constraints.

An important aspect of calculations on noncubic materials is that, in general, it is not possible to derive a central-force potential for which the crystal is fully in equilibrium with the observed structure. Therefore, in

defect calculations which relax a region of the crystal (region I) around the defect, some of the relaxation energy is attributable to relaxation of the perfect lattice, and not due to the effect of the defect. This problem may be overcome by estimating the relaxation energy of region I, in the absence of the defect; the resulting energy is then subtracted from the calculated defect energy to give the true energy. An alternative, simpler procedure is to relax the whole crystal structure to equilibrium before performing the defect calculations. In the present paper we report energies obtained using the former procedure, although we found no significant differences when calculations were repeated using the latter method.

The calculations were mostly performed on the Cray Research, Inc. 1s computer at the University of London Computer Centre, London, United Kingdom, although those involving migration energies were carried out on a Digital Equipment Corporation VAX11/780 computer at the New York State College of Ceramics and at the Cornell National Supercomputer Facility. An inner region I containing between 120 and 150 ions was used for all the calculations; experience has indicated that fewer ions in region I do not permit complete equilibration of the crystal. We note in passing that the lower tetragonal symmetry of the rutile structure means that the memory requirements for these calculations are greater than would be necessary for similar calculations on crystals with cubic symmetry.

It is well established that the reliability of the results of modern defect simulations is largely dependent on the quality of the interatomic potentials employed. In the present study, we used standard Born model potentials with integral ionic charges and the shell model to represent ion polarizability (for a more detailed discussion, see Ref. 9). The analytical form of the potential is written

$$V_{ij}(r_{ij}) = \frac{q_i q_j}{r_{ij}} + A_{ij} \exp\left[-\frac{r_{ij}}{\rho_{ij}}\right] - C_{ij} r_{ij}^{-6},$$

where the parameters  $A_{ij}$ ,  $\rho_{ij}$ , and  $C_{ij}$  are optimized for each particular interaction. Details of the parameters and the physical properties calculated for  $\text{MnF}_2$  and  $\text{MgF}_2$  are found in the Appendix.

Because charged defects will polarize other ions in the crystal, ion polarizability must be incorporated into the potential model. In our case, this is done through use of the shell model of Dick and Overhauser.<sup>10</sup> In this simple, but effective model, the ion is composed of a core (representing the nucleus and core electrons) and a shell (representing the valence electrons). The total, formal, charge on the ion is divided between the core and shell in such a way as to reproduce the ion polarizability, given in the model by  $\alpha = Y^2/k$ , where  $Y$  is the shell charge and  $k$  is the harmonic spring constant coupling the core and shell. The effectiveness of this model can be gauged by comparing the calculated and observed dielectric constants given in the Appendix. Short-range forces were taken as acting between cations and anions, and between anions and anions; cation-cation short-range interactions were neglected, an approximation we consider to be

justified, given the large cation-cation separations in the crystals. The F-F short-range potential parameters used in the calculations are similar to those employed by Catlow *et al.*<sup>4</sup> in their study of the alkaline-earth fluorides. Because this potential was fitted to the properties of all three alkaline-earth fluorides with the fluorite structure, a range of F-F separations is sampled and we feel very confident about its validity. The only difference is that we found it more convenient to use the straightforward Buckingham potential rather than the splined form. In the previous work of Catlow *et al.*,<sup>4</sup> the F-F potential parameters were included, along with the M-F parameters, in the fit to the crystal properties. In the present case, only the M-F parameters were varied, and were found by empirical fitting procedures, using the measured elastic and dielectric constants. The resulting parameters, together with the calculated and experimental crystal data are reported in the Appendix. We note that an earlier theoretical study on  $\text{MnF}_2$  and  $\text{MgF}_2$  by Cran and Sangster<sup>11</sup> used a force-constant model to obtain elastic, dielectric, and phonon properties. Such a model cannot, however, be used to obtain defect energies.

### III. RESULTS

#### A. Intrinsic disorder

Defect-formation energies for cation and anion vacancies and for anion interstitials are given in Table I. They have been corrected for the residual relaxation energy discussed in Sec. II, the value of which is also given, for an inner region I containing 150 ions. By considering the quasicheical defect-formation reactions, the energies of Frenkel pairs and Schottky trios may be obtained. For example, the anion Frenkel formation reaction takes a lattice anion,  $F_F$  from its regular site, creating an intersti-

TABLE I. Defect-formation energies.

Defect	$\text{MnF}_2$	
	Energy (eV) <sup>a</sup>	
$V_{\text{Mn}}$	23.11	
$V_{\text{F}}$	5.52	
$F_i$ , tetrahedral	-2.39	
$F_i$ , octahedral	-2.27	
$F_i$ , split	-2.46	
Defect	$\text{MgF}_2$	
	Energy (eV) <sup>b</sup>	
$V_{\text{Mg}}$	25.56	
$V_{\text{F}}$	6.21	
$F_i$ , tetrahedral	-1.22	
$F_i$ , octahedral	-1.29	
$F_i$ , split	-1.32	

<sup>a</sup>Corrected for residual relaxation energy of 0.48 eV (see text).

<sup>b</sup>Corrected for residual relaxation energy of 0.22 eV (see text).

tial ion  $F_i$  and an anion vacancy  $V_F$  to give the following reaction:



(Schottky energies also require the calculated lattice energy of the crystals reported in the Appendix along with the other crystal data.) The results are compared in Table II with those of the earlier study.<sup>5</sup>

In the case of anion interstitials, three models were considered, viz., octahedral and tetrahedral interstitial sites and a split-interstitial configuration. This latter defect structure, shown in Fig. 1(b), consists of two  $F^-$  ions

TABLE II. Intrinsic disorder energies.

Type of disorder	Energy per defect (eV)			
	MnF <sub>2</sub>		MgF <sub>2</sub>	
	(a)	(b)	(a)	(b)
Schottky	1.99	1.83 <sup>c</sup>	2.89	2.19 <sup>c</sup>
Anion Frenkel	1.53	1.94	2.44	2.55
Cation Frenkel	3.09	2.78	4.56	3.75

<sup>a</sup> Present study.

<sup>b</sup> From Catlow *et al.* (Ref. 5).

<sup>c</sup> In the original paper (Ref. 5) the Schottky energy, which was reported as the triplet, was, in fact, the energy per defect.

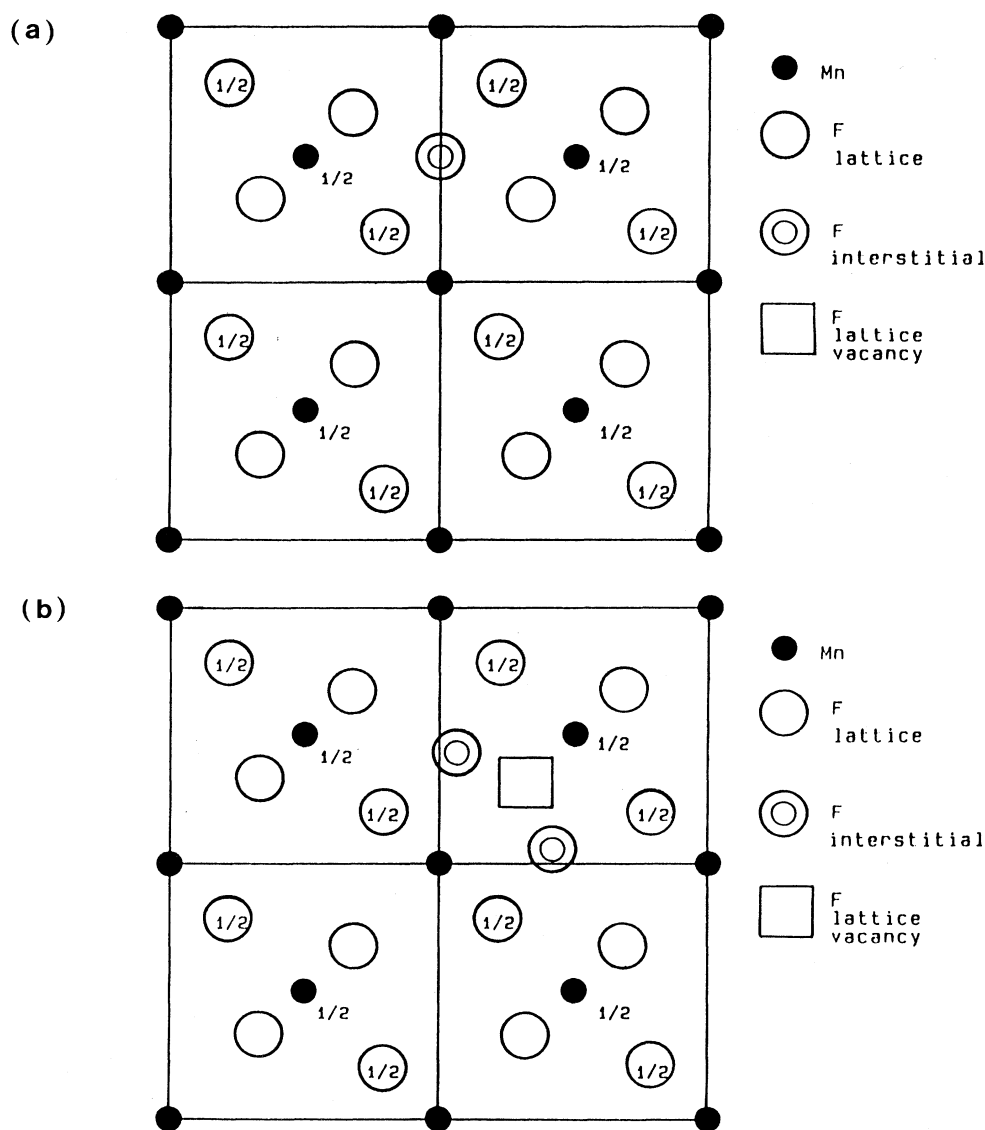


FIG. 1. Projection of the rutile structure on (001): (a) showing the position of a simple  $F^-$  interstitial at  $(\frac{1}{2}, 0, 0)$  and (b) showing the structure of a split-interstitial defect. The presence of the interstitial near  $(\frac{1}{2}, 0, 0)$  has caused the lattice anion at  $(u, u, 0)$  ( $u \sim 0.3$ ) to be displaced towards  $(0, \frac{1}{2}, 0)$ .

occupying octahedral interstitial sites neighboring an anion vacancy. This configuration occurs because the introduction of a single  $F^-$  ion into an octahedral interstitial position causes the neighboring lattice anion to be displaced into another interstitial position, resulting in two interstitial species and a vacancy. There is still only a net of one interstitial ion, but now it is split between two sites—hence the description “split interstitial.”

The energies of the three configurations are very similar—a result which has considerable consequences for the interpretation of  $F^-$ -ion migration in the material. The calculated Frenkel energies reported were obtained using the split-interstitial energy, which is marginally favored for both crystals. (In fact, as the size of region is increased, the split-interstitial structure becomes more stable relative to the simple interstitial configurations.) The two anions in the split interstitial were found to remain on the  $z=0$  mirror plane [which is the (001) plane that contains the cation], in spite of repeated efforts to find a lower-energy asymmetrical configuration. This is significant in the light of our later results for the structure of this complex in the presence of foreign or dopant cations, which we discuss below.

### B. Dopant energies and defect structure

In this subsection we discuss the energy and structure of defects associated with dopants. For  $MnF_2$  the dopants considered are  $Er^{3+}$  and  $Y^{3+}$ , while for  $MgF_2$  we looked at a  $Sc^{3+}$  dopant. In these three cases the binding energy and structure of the dopant and compensating F interstitial were examined for a low-symmetry configuration. In addition, because Schottky disorder would give rise to a compensating cation vacancy, the structure of an Er dopant and  $V_{Mn}$  complex (in  $MnF_2$ ) was calculated to see if this might also provide an explanation for the relaxation peaks described in the previous paper.<sup>1</sup> In spite of removing all symmetry constraints, the structure around the  $(Er_{Mn} \cdot V_{Mn})$  complex retained its natural lattice symmetry. This result has two consequences. First, it cannot be used to explain the relaxation effects described earlier,<sup>1</sup> and second, it adds support to our conclusion that anion Frenkel, rather than Schottky, disorder dominates in this material.

Next, we consider the interaction between the dopants,

$Er^{3+}$  and  $Y^{3+}$  with a  $F^-$  interstitial, in  $MnF_2$ . We recall that the structure of the anion interstitial involves more than a single interstitial species (being a split interstitial), and hence we would expect the structure of the dopant-interstitial complex to be similar, especially given the relaxation effects that have been observed experimentally in doped crystals. As we shall see, the computer-simulation techniques offer an insight into the atomistic mechanism underlying the observed relaxation effects that are difficult to obtain by other means. First of all, we examined the energy of the dopant interacting with a simple interstitial, then with the split-interstitial configuration, and then, third, with the two  $F^-$  ions displaced in an asymmetric fashion (one above and one below) from the  $z=0$  mirror plane. This last structure was found to have the lowest energy, although as the ions are symmetrical with respect to the  $(1\bar{1}0)$  mirror plane, this defect structure does not have an asymmetry consistent with the relaxation peaks seen by Ling and Nowick.<sup>1</sup>

Therefore, a lower-symmetry configuration was deliberately sought. In this calculation any remaining symmetry was removed completely by suitably distorting the initial configuration. The resulting equilibrium structure of this defect had the same energy as the previous low-symmetry structure, but was clearly a different structure, now being asymmetrical both parallel and perpendicular to  $c$ . The coordinates of these configurations are reported in Table III, and the dopant-interstitial binding energies are summarized in Table IV. Note that only one energy for each dopant in  $MnF_2$  is given, because *both* off-the-mirror-plane asymmetric configurations have the same calculated energy.

In the isolated, split-interstitial, structure (in the absence of dopants) the F interstitials remain in the basal mirror plane; thus the low-symmetry structures just described are only predicted to occur in doped  $MnF_2$  samples, not in the pure material. This result also matches the experimental findings in the previous paper.<sup>1</sup>

Finally, we set up a similar low-symmetry configuration for a split interstitial—the scandium dopant in  $MgF_2$ . In this case, however, the F ions in the defect complex returned to the mirror plane, indicating a different behavior for Sc-doped  $MgF_2$  compared to doped  $MnF_2$ .

The asymmetric configuration (a) in Table III meets

TABLE III. Low-symmetry dopant-interstitial defect configurations. The origin is taken as the position of the unrelaxed dopant ion.

Species	Asymmetric dipolar configuration			Symmetric off-mirror plane configurations		
	$x$	$y$	$z$	$x$	$y$	$z$
$Er_{Mn}$	0.017	0.037	0.004	0.031	0.031	0.00
F	0.462	0.193	-0.037	0.483	0.138	-0.063
F	0.075	0.487	0.103	0.138	0.483	0.063
$Y_{Mn}$	0.013	0.036	0.006	0.029	0.029	0.0
$F_i$	0.439	0.191	-0.059	0.462	0.126	-0.073
$F_i$	0.053	0.461	0.117	0.126	0.462	0.073

TABLE IV. Dopant-anion interstitial interaction energies.

MnF <sub>2</sub>	Binding energy (eV)	
	(a)	(b)
Er-F <sub>i</sub>	0.90	0.94
Y-F <sub>i</sub>	0.73	0.80
MgF <sub>2</sub>	Binding energy (eV)	
Sc-F <sub>i</sub>	1.56	

<sup>a</sup> On-the-mirror-plane configuration.

<sup>b</sup> Asymmetric configuration.

the requirement for an off-symmetry defect to account for the low-temperature dielectric relaxation results of paper I. It is a triclinic defect that is asymmetric both with respect to the (001) and the (1 $\bar{1}$ 0) planes. Accordingly, it can give rise to relaxation in orientations both parallel and perpendicular to the *c* axis. The small displacements of the two F<sub>*i*</sub> ions from the (001), or *z* = 0, plane also suggest that the activation energy for reorientation parallel to the *c* axis is extremely low. Thus, these calculations accord very nicely with the experimental result on Er- and Y-doped MnF<sub>2</sub>.<sup>1</sup> Note that the energy differences in Table IV would have to be resolved into their components parallel and perpendicular to the *c* axis in order to compare with the activation energies for dielectric relaxation reported in paper I.<sup>1</sup> The magnitude of these energies lies at the limits of accuracy attainable with the current set of interatomic potentials and so this resolution was not done. However, the calculated atomic configuration can be used to estimate the dipole moments; in this case, the calculations predict  $p_{\perp} > p_{\parallel}$  as discussed in paper I.<sup>1</sup>

### C. Migration energies

We have considered three different sets of migration mechanisms: those involving cation vacancies, those involving anion vacancies, and those involving anion inter-

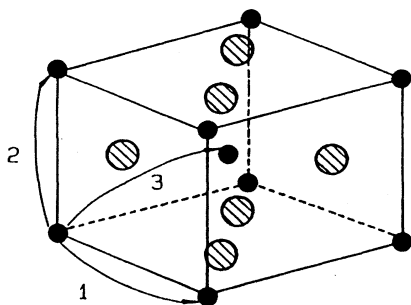


FIG. 2. Diagram of rutile unit cell showing the cation-vacancy migration paths referred to in the text and Table V.

TABLE V. Migration energies in MnF<sub>2</sub>.

Cation-vacancy mechanisms [Fig. 2(a)]	
Jump direction	Energy (eV)
[100]	1.18
[001]	1.33
[111]	1.37
Anion-vacancy mechanisms [Fig. 2(b)]	
Jump	Energy (eV)
(1)	0.40
(2)	1.07
(3)	0.91
Anion-interstitial mechanisms	
Jump mechanism	Energy (eV)
along [001]	0.19
in <i>a-b</i> plane	0.12
(saddle-point site: $\frac{1}{2}, 0, 0$ )	

stitials. Although the latter are the most significant, given our findings for the intrinsic disorder, we report the calculated energies for the others for the sake of completeness.

#### 1. Cation-vacancy mechanisms

As illustrated schematically in Fig. 2, there are three possible paths: along [100], [001], and [111], labeled 1, 2, and 3, respectively. The energies which we report in Table V are all quite high, being between 1.1 and 1.4 eV, the lowest along [100]. The difference between these energies is not very great, suggesting that the ionic-related migration anisotropy will also not be great.

#### 2. Anion-vacancy mechanisms

From Fig. 3 we again see that there are three possible mechanisms involving anion vacancies, labeled 1, 2, and 3. The lowest energy (Table V) is found for the jump labeled 1, although this, in fact, cannot lead to long-range transport by itself. Thus the activation energy for anion-

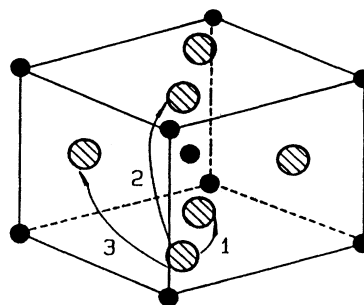


FIG. 3. Diagram of rutile unit cell showing the anion-vacancy migration paths referred to in the text and Table V.

vacancy migration is expected to be of the order of 1 eV, that found for jump 2. Jump 3, which involves components in both the  $a$  and  $c$  directions, was of too low a symmetry for calculation on the VAX11/780 computer, so this calculation was performed at the Cornell University National Supercomputer Facility (NSF). The energy reported here assumes that the saddle-point site is (0.555, 0.25, 0.25). The energies at a number of positions (about 15) near this site were obtained to support this assumption, and there was no evidence to suggest that the migration path would be radically different from the one assumed.

### 3. Anion-interstitial mechanisms

Here there are two jump mechanisms of interest. First, there is the migration path along the  $c$ -axis channels in the rutile structure, and secondly there is the migration in the basal plane to be considered. Our calculations of the  $F^-$ -ion interstitial energy indicate that the saddle-point position for transport along the  $c$  axis would be the octahedral site which lies in the basal plane. This has a higher energy than the tetrahedral position at  $z = \frac{1}{4}$ . The activation energy is thus the difference between the energies of the split-interstitial ground state and the octahedral site.

For transport in the basal plane, a natural mechanism is suggested by the split-interstitial configuration. Moving the split interstitial from one unit cell to the next involves a saddle-point configuration, which is just the simple octahedral  $F^-$ -ion interstitial; again, the activation energy is the difference between the energies of these two configurations.

How do these results fit with the interpretation by Ling and Nowick, from their conductivity data, of a single interstitialcy mechanism? The two mechanisms just described may be considered as components of the interstitialcy mechanism which involves moving a split interstitial from a unit cell at  $z = 0$  to an adjacent unit cell at a position  $z = \frac{1}{2}$ . The saddle-point configuration or the interstitialcy mechanism would have the  $F^-$  ion in the tetrahedral position in the  $c$ -axis channel; in addition, there would be some displacement of the lattice anions involved in either split-interstitial structure. A calculation of the energy of this saddle-point configuration would be quite difficult. The low symmetry would entail a lengthy computation and several of these would be necessary to ensure that the true saddle point had been found. Such a set of calculations was not thought to be really useful. Rather, the activation energies of the two simple mechanisms were considered to be representative of the energy of the interstitialcy mechanism itself. Clearly the simulations and experiment are in agreement over the very low magnitude of  $F^-$ -ion transport in this material.

## IV. DISCUSSION

Our results are quite different to the earlier work,<sup>5</sup> most significantly in the prediction of the dominant mode

of intrinsic disorder, which we now consider to be of anion Frenkel type, instead of Schottky. Comparison between the defect energies obtained in this study with those reported earlier shows that the major change is in the value of the Frenkel energy. The difference between the two sets of calculations can be attributed almost entirely to the changes in the F-F short-range potential: those used in the earlier study are too repulsive and softening the potential has led to a lowering of the interstitial energy. The results show the sensitivity of calculated interstitial energies to potential parameters in close packed and nearly close-packed crystal structures, such as the rutile structure. This sensitivity contrasts with a much weaker dependence on potentials that was found in the studies of the alkaline-earth fluorides,<sup>4</sup> which have a more open structure.

Quantitative comparison between theoretical and experimental defect energies is only possible for the case of  $MnF_2$  at present; analyses of conductivity data give values of 1.77 eV per defect for the most favorable mode of intrinsic disorder.<sup>1</sup> Our calculations suggest this will be of anion Frenkel type, for which our calculated energy of 1.53 eV (per defect) is in satisfactory agreement with that measured.

Furthermore, assuming this defect structure, our calculated activation energies of approximately 0.1–0.2 eV are in excellent agreement with those deduced from the conductivity data, which also find very low values of 0.1 eV, both parallel and perpendicular to the unique axis.

In our study of the doped systems, the most significant result is the prediction of a low-symmetry dipolar configuration in the case of doped  $MnF_2$ , but not in undoped  $MnF_2$ , nor in  $MgF_2$ , either undoped or with Sc dopants. Such behavior accords with what has been found experimentally so far.<sup>1</sup>

In conclusion, this work clearly shows the potential benefits of detailed computer-simulation studies in elucidating atomistic mechanisms of ion transport and defect behavior in complex systems. The method is at its most powerful when combined with experimental studies, as this present paper demonstrates.

The results also emphasize the need for reliable anion-anion potential parameters when studying interstitial defect structures, especially in close-packed materials.

## ACKNOWLEDGMENTS

We thank the North Atlantic Treaty Organization (NATO) for a travel grant and are grateful to Alfred University, the University of London, and Columbia University for the provision of computing facilities. Those from Columbia University were supported by a grant from the U.S. Department of Energy (DOE). Part of this work was performed at the Cornell National Supercomputer Facility, which is funded in part by the National Science Foundation (NSF), New York State, and IBM Corporation, whose support we are pleased to recognize. Profitable discussions with Professor A. S. Nowick must not go unmentioned.

## APPENDIX

The potential parameters and crystal properties of the interatomic potential models for (a)  $\text{MnF}_2$  and (b)  $\text{MgF}_2$  are presented below.

(a) Interatomic potential model for $\text{MnF}_2$				(b) Interatomic potential model for $\text{MgF}_2$			
Potential parameters	Crystal properties			Potential parameters	Crystal properties		
	Expt. <sup>a</sup>	Calc.			Expt. <sup>a</sup>	Calc.	
$A_{+-} = 1031.0$	$C_{11}$	10.3	9.8	$A_{+-} = 682.59$	$C_{11}$	13.99	13.59
$\rho_{+-} = 0.293\ 51$	$C_{12}$	8.2	7.8	$\rho_{+-} = 0.297\ 97$	$C_{12}$	8.93	9.59
$C_{+-} = 0.0$	$C_{13}$	7.1	6.1	$C_{+-} = 0.0$	$C_{13}$	6.37	6.19
$A_{\text{FF}} = 1127.7$	$C_{33}$	16.3	17.1	$A_{\text{FF}} = 1127.7$	$C_{33}$	20.42	23.19
$\rho_{\text{FF}} = 0.2753$	$C_{44}$	3.0	3.5	$\rho_{\text{FF}} = 0.2753$	$C_{44}$	5.7	5.25
$C_{\text{FF}} = 15.8$	$C_{66}$	6.8	7.8	$C_{\text{FF}} = 15.8$	$C_{66}$	9.54	9.63
$Y_{\text{Mn}} = 10.735$	$\epsilon'_0$	8.9	8.9	$Y_{\text{Mg}} = 2.000$	$\epsilon'_0$	5.5	5.63
$K_{\text{Mn}} = 1380.622$	$\epsilon''_0$	7.4	7.4	$K_{\text{Mg}} = 9\ 999\ 999.9$	$\epsilon''_0$	4.82	4.55
$Y_{\text{F}} = -1.6395$	$\epsilon'_\infty$	2.2	3.3	$Y_{\text{F}} = -1.233\ 57$	$\epsilon'_\infty$	1.9	1.90
$K_{\text{F}} = 20.908$	$\epsilon''_\infty$	2.2	3.5	$K_{\text{F}} = 17.496$	$\epsilon''_\infty$	1.9	1.90
	lattice energy	-56.98	-56.36		lattice energy	-60.74	-59.075
	(residual lattice strains: $a = 0.8\%$ , $c = -2.8\%$ )				bulk strains	0.7%	-4.2%

<sup>a</sup> From Refs. 12 and 13.

\*Present address: Corporate Research Science Laboratories, Exxon Research and Engineering Company, Clinton Township, Route 22 East, Annandale, NJ 08801.

<sup>1</sup>S. Ling and A. S. Nowick, this issue, the preceding paper, *Phys. Rev. B* **40**, 3266 (1989).

<sup>2</sup>C. R. A. Catlow, K. M. Diller, and M. J. Norgett, *J. Phys. C* **10**, 1395 (1977).

<sup>3</sup>C. R. A. Catlow and M. J. Norgett, *J. Phys. C* **6**, 1325 (1973).

<sup>4</sup>C. R. A. Catlow, M. J. Norgett, and T. A. Ross, *J. Phys. C* **10**, 1627 (1977).

<sup>5</sup>C. R. A. Catlow, R. James, and M. J. Norgett, *J. Phys. (Paris) Colloq.* **37**, C7-443 (1976).

<sup>6</sup>M. Leslie, Science and Engineering Research Council (U.K.)

Daresbury Laboratory, Technical Memorandum No. SCI/DL/TM31T, 1982 (unpublished).

<sup>7</sup>C. R. A. Catlow, R. James, W. C. Mackrodt, and R. F. Stewart, *Phys. Rev. B* **25**, 1006 (1982).

<sup>8</sup>*Computer Simulation of Solids*, Vol. 166 of *Lecture Notes in Physics*, edited by C. R. A. Catlow and W. C. Mackrodt (Springer-Verlag, Berlin, 1982).

<sup>9</sup>See Ref. 8, Chap. 7.

<sup>10</sup>B. G. Dick and A. W. Overhauser, *Phys. Rev.* **112**, 90 (1958).

<sup>11</sup>G. C. Cran and M. J. L. Sangster, *J. Phys. C* **7**, 1937 (1974).

<sup>12</sup>S. Haussuhl, *Phys. Stat. Solids* **28**, 127 (1968).

<sup>13</sup>G. Parisot, *C. R. Acad. Sci. Paris Ser. B* **265**, 1192 (1967).